

**Fast formation and superconductivity of MgB₂ thick films grown on stainless steel
substrate**

A.H. Li, X.L. Wang, M. Ionescu, S. Soltonian, J. Horvat, T. Silver, H.K. Liu, and S.X. Dou

Institute for Superconducting and Electronic Materials, University of Wollongong, NSW
2522, Australia

(Submitted to Physica C on 3/27/2001, Received on 4/10/2001, Revised on 4/24/2001)

Abstract

The fabrication, characterisation, and superconductivity of MgB₂ thick films grown on stainless steel substrate were studied. XRD, SEM, and magnetic measurements were carried out. It was found that the MgB₂ thick films can be fast formed by heating samples to 660 °C then immediately cooling down to room temperature. XRD shows above 90% MgB₂ phase and less than 10 % MgO. However, the samples sintered at 800 °C for 4 h contain both MgB₄ and MgO impurities in addition to MgB₂. The fast formed MgB₂ films appear to have a good grain connectivity that gives a J_c of 8 x 10⁴ A/cm² at 5 K and 1 T and maintained this value at 20 K in zero field.

Introduction

The discovery of superconductivity at 39 K in MgB₂ [1] has generated great interest worldwide in both fundamental studies and practical applications worldwide. Critical current densities on the order of 10^4 to 10^5 A/cm² have been reported by several groups for polycrystalline MgB₂ bulk samples [2-8]. A strong link type critical current density has been observed, regardless of the degree of grain alignment [3]. This would be an advantage for making wires or tapes with no degradation of J_c, unlike the degradation due to the grain boundary induced weak-links which is a common and a serious problem widely encountered in cuprate high temperature superconductors. H_{c2} of MgB₂ has been determined to be as high as 14 T at 4.2 K. A significantly large J_c of 10^6 A/cm² at 4.2 K and 1 T and enhancement of the irreversibility line have been reported in high quality epitaxial MgB₂ thin films grown on Al₂O₃ and SrTiO₃ single crystal substrates [9, 10]. This result gives further encouragement of to the development of MgB₂ for high current applications. Fabricating MgB₂ into tapes or wires will be essential for most such applicants. The first short wire of MgB₂ reported was made by exposing boron filament to magnesium vapour [11], with a J_c of 10^5 A/cm². For tape fabrication, it is very important to find a suitable sheath material for MgB₂ which does not degrade the superconductivity. The first tape of MgB₂ reported was made using Nb as sheath material [12]. The motivation for our study on the fabrication of MgB₂ thick films on different substrates is to find a suitable sheath material for making MgB₂ tapes, as thick film preparation is very much easier than making tapes. In addition, the thick films of MgB₂ have a great potential for applications in magnetic shielding devices and high power microwave devices that will work at significantly higher temperatures than conventional low T_c superconductors, due to the high T_c of 39 K. It was reported very recently that the surface

resistance of a dense MgB_2 sample is lower than that of polycrystalline Y-123 bulks and matches with Y123 single crystals [13]. These results show promise for the use of MgB_2 in microwave applications. We have noted that there are plenty of elements in the periodic table that can form the AlB_2 structure, and that most of them have a high solubility in MgB_2 [14]. Because the supercurrent is most likely carried by holes, any electron doping reduce the hole concentration level and in turn degrades the T_c of MgB_2 [15]. It has been shown that doping can degrade the T_c in $\text{Mg}_{1-x}\text{Al}_x\text{B}_2$ [16]. It is noted that the size of iron is very small compared with Mg and therefore the ion has a very small solubility in MgB_2 . In this letter, we report our study on the formation and properties of MgB_2 thick films grown on stainless steel substrate.

Experimental

For the film preparation, a suspension of mixed magnesium and amorphous boron powder was made by stirring the powders together with acetone. The powders of Mg and B were deposited suspension after evaporation of acetone on a piece of polished stainless steel which placed at the bottom. This procedure was repeated several times until the desired thickness was reached. The resulting samples were pressed under high pressure after the deposition process in order to increase the density of the deposited films. Another piece of stainless steel of the same size as the substrate was placed onto the top of the deposited films so as to avoid the loss and oxidation of Mg during the sintering at high temperatures.

The samples were sintered in a tube furnace using two different temperature profiles (a) and (b) as shown in Fig. 1. For (a), the temperature was increased at a heating rate of $300\text{ }^\circ\text{C/h}$ to $660\text{ }^\circ\text{C}$, which is the exact melting point of magnesium, then furnace cooled down to room temperature without any holding period at $660\text{ }^\circ\text{C}$. For (b), temperature was increased at the

same heating rate of 300 °C/h to 800 °C, and held there for 4 h, then furnace cooled down to room temperature. A flow of high purity Ar gas was maintained throughout the whole sintering process.

The phases and film morphologies were investigated using X-ray diffraction (XRD) and scanning electron microscopy (SEM). Superconductivity was characterised using PPMS. The superconducting transition temperature was determined by measuring ac susceptibility as a function of temperature. Magnetisation hysteresis loops were recorded at 5 K and 20 K in fields up to 8 Tesla.

Results and discussion

After removing the top piece of stainless steel, the films were found to be of a shining with black colour. However, the films appear not to be firmly attached to the substrate. A plate-like layer of film could be easily removed from the substrate, probably indicative a non-reaction between the films and the stainless steel. This can be understood by considering that iron has a very small solubility in MgB₂ due to the fact that the iron is too small compared with the Mg. Another reason for the poor adherence of the film to the substrate is the formation of fine particles of MgO that may be acting as a barrier. This is evidenced by the SEM result as will be seen below. It is also possible that there may be a large difference in thermal expansion at high temperatures for steel and MgB₂ so that they separate from each other during cooling.

The thicknesses of the films are about 160 μm. The density of both samples is about 1.6g/cm³.

Fig.2 shows the XRD patterns for samples sintered by temperature profile (a) (sample A) and (b) (sample B). It can be seen that most of the peaks can be indexed using the lattice

parameters of MgB_2 . Sample A only contains MgO impurities. However, sample B which was sintered at $800\text{ }^\circ\text{C}$ for 4 h, contains both MgO and MgB_4 . This means that heating up to $660\text{ }^\circ\text{C}$ without further holding time is sufficient for MgB_2 phase formation for the full amount of materials used in the films. According to the Mg-B phase diagram, MgB_2 can decompose to MgB_4 only at high temperatures above $1545\text{ }^\circ\text{C}$ [17]. The sintering temperature of $800\text{ }^\circ\text{C}$ used for sample B is much lower than the decomposition temperature of MgB_2 , but it is much higher than the melting point of magnesium. Therefore, it is very likely that some of the magnesium evaporated at $800\text{ }^\circ\text{C}$ through the flow of Ar gas at the early stage of the reaction between magnesium and boron. This loss of magnesium at $800\text{ }^\circ\text{C}$ would have caused a change of the stoichiometry from the starting composition to the magnesium poor or boron rich side, which in turn resulted in the formation of MgB_4 in addition to MgB_2 as indicated in the phase diagram [14][17]. The formation of MgO may come from the starting Mg which may contain MgO.

Fig. 3 shows the SEM images of the two samples. Sample A shows a flat and dense surface (Figs 3(a) and (b)) with grain sizes of less than $1\text{ }\mu\text{m}$. Sample B (fig. 3 (c)) had a rougher surface but similar grain size. The cracks seen in Fig. 3 (a) mainly occurred after handling. Fig. 3 (d) is the surface of the substrate after the MgB_2 film was removed. The grains from substrate are clearly seen with some small white MgO particles on top of them. The formation of MgO may be a barrier to the adherence of film to the substrate.

The T_c of 37.5 K was determined for both samples by using a.c. susceptibility in an ac field of 1 Oe and a frequency of 117 Hz , as shown in Fig. 4. Both samples have a similar value of

susceptibility. M-H loops measured at 5 and 20 K for both samples are shown in Fig. 5. A flux jump for $H < 1$ T can be seen for both samples at 5 K which is the same as what has been reported for a MgB_2 pellet with grain sizes as large as $200 \mu\text{m}$ [18]. In addition, the magnetisation hysteresis is much larger than for a weak-linked MgB_2 sample which was sintered at 800°C using high pressure and reacted MgB_2 powders used as starting material [19]. This means that the grains are well connected, similar to what is formed in compacted MgB_2 pellets with large grain sizes of about $200 \mu\text{m}$ [18]. The critical current density can be obtained from the loops using the formula $J_c = 20 \text{ M/a}(1-a/3b)$ ($a < b$) [20]. The J_c as a function of temperature is shown in Fig. 6. The J_c at 5 K for $H < 1$ T cannot be defined due to the flux jump. The J_c of both samples is about $8 \times 10^4 \text{ A/cm}^2$ at 5 K and 1 T and 7×10^4 and 10^5 A/cm^2 at 20 K and zero field for samples A and B, respectively. J_c for sample A is thus the same order as for sample B. This value is larger than for Nb sheathed MgB_2 tape which has a J_c of $4.2 \times 10^4 \text{ A/cm}^2$ at 4.2 K and 1 T [12].

Although the MgB_2 thick films in our present work does not firmly attached to the steel substrate, it should be noted that the sintering conditions relating to cooling, heating rate and holding time still cannot be considered optimum. The situation might be different in iron sheath MgB_2 tapes. We have found that the MgB_2 can strongly adhere to iron sheath materials. A thin layer of iron might be a suitable buffer layer between MgB_2 and other metal sheath materials which could react with MgB_2 . For example, copper, which reacts with Mg and MgB_2 and form MgCu_2 at high temperatures [20], could be coated with a very thin layer of iron. Composite of this type is under fabrication in our group.

Conclusions

The MgB₂ thick films on stainless steel substrate can be fast formed by heating samples to 660 °C without any holding and quickly cooled down. XRD show above 90% MgB₂ phase. However, the samples sintered at 800 °C for 4 h contains MgB₄ and MgB₂ and MgO. The fast formed MgB₂ films appear to have a good grain connectivity that gives a J_c of 8 x 10⁴ at 5 K and 1 T and maintained this value at 20 K in zero field. However, the MgB₂ films are not well adherent to steel substrate. The most possible reason may be big difference in thermal expansion coefficient between them. It is possible that a thin layer of ion can be used a buffer layer in other metallic sheath materials to MgB₂.

Acknowledgments

This work is partly support by the funding from Australian Research council and University of Wollongong.

References

1. Jun Nagamatsu, Norimasa Nakagawa, Takahiro Muranaka, Yuji Zenitani and Jun Akimitsu. *Nature*, 410 (2001) 63
2. Takano Y, Takeya H, Fujii H, Kumakura H, Hatano T, and Togano K., *Cond-mat/01020167*
3. Larbalestier D.C, Rikel M. O, Cooley L. D, Polyanskii A.A, Jiang J. Y, Patnaik S, Cai X.Y, Feldmann D. M, Gurevich A, Squitieri A. A, Naus M. T, Eom C. B, Hellstrom E. E. *Nature*, 410 (2001) 186
4. Bugoslavsky Y, Perkins G. K, Qi X, Cohen L. F, and Caplin A. D. , *Cond-mat/0102353*
5. Kim Mun-Seog, Jung C. U, Park Min-Seok, Lee S. Y, Kim Kijoon H. P, Kang W. N, and Lee Sung-Ik, *Cond-mat/0102338*
6. Wen H. H, Li S. L, Zhao Z. W, Ni Y. M, Ren Z. A, Che G. C, Yang H. P, Liu Z. Y, and Zhao Z. X., *Cond-mat/0102436*
7. Muller K.-H, Fuchs G, Handstein A, Nenkov K, Narozhnyi V. N, Eckert D., *Cond-mat/0102517*
8. Kim Kijoon H. P, Kang W. N, Kim Mun-Seog, Jung C. U, Kim Hyeong-Jin, Choi Eun-Mi, Park Min-Seok, and Lee Sung-Ik, *Cond-mat/0103176*
9. Kang W. N, Kim Hyeong-Jin, Choi Eun-Mi, Hung C. U, Lee Sung-Ik, *cond-mat/0103179*
10. C.B. Eom, et al., *cond-mat/0103425*, submitted to *Nature*
11. Canfield P. C, Finnemore D. K, Bud'ko S. L, Ostenson J. E, Lapertot G, Cunningham C. E, and Petrovic C, *Phys. Rev. Lett.*, 86 (2001) 2423
12. Sumption M. D, Peng X, Lee E, Tomsic M, and Collings E. W., *Cond-mat/0102441*
13. N.Hakim, et al., *cond-mat/0103422*

14. T. Massalski, ed., Binary Alloy Phase Diagrams (A.S.M International, Materials Park, OH), 2nd ed. 1990
15. Hirsch J. E., Cond-mat/0102115
16. J.S. Slusky, N. Rogado, K.A. Regan, M.A. Hayward, P. Khalifah, T. He, K. Inumaru, S.M. Loureiro, M.K. Haas, H.W. Zandbergen, and R.J. Cava, Nature 410 (2001) 343
17. Z.K. Liu, D.G. Schlom, Q.Li, X.X. Xi, Cond-mat/0103335
18. S.X. Dou, X.L. Wang, J. Horvat, D. Milliken, E.W. Collings, and M.D. Sumption, cond-mat/0102320
19. Kang W. N, Jung C. U, Kim Kijon H. P, Park Min-Seok, Lee S. Y, Kim Hyeong-Jin, Choi Eun-Mi, Kim Kyung Hee, Kim Mun-Seog, and Lee Sung-Ik, cond-mat/0102313
20. P.S. Swartz and C.P. Bean, J. Appl. Phys., 39 (1968) 4991
21. S.X. Dou, et al., unpublished

Figure captions

Fig.1. Temperature profile for sample A (a) and sample (b).

Fig. 2. XRD for samples A (a) and B (b).

Fig 3. SEM surface images of samples A: (a) and (b) and B (c) and substrate (d). The magnification scale is the same in (c) and (d).

Fig.4. Temperature dependence of ac susceptibility of MgB_2 thick films for sample A (open circles) and B (solid line) after removal from the substrate.

Fig.5. Magnetisation hysteresis loops measured at 5 and 20 K. Open (5K) and closed circles (20K) represent sample A, and solid (5K) and dashed (20K) lines represent sample B.

Fig. 6. J_c vs magnetic field. The symbols have the same meanings as in figure 4. The arrow shows the maximum field where the flux jumping ends.

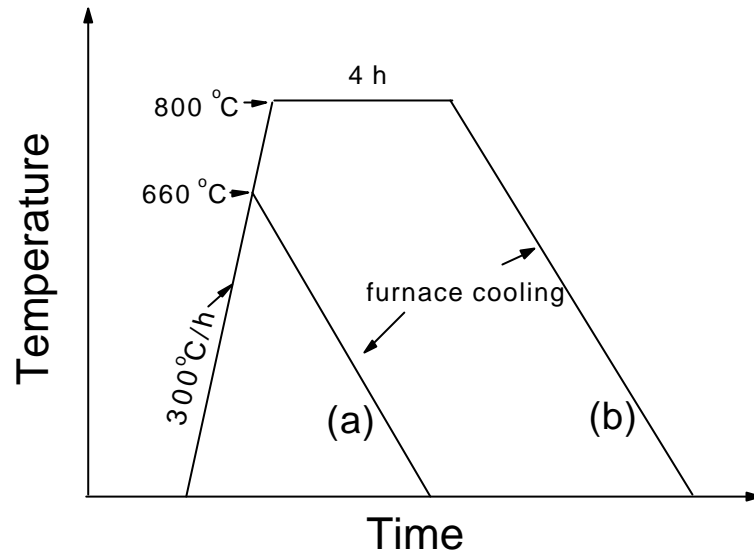


Fig. 1

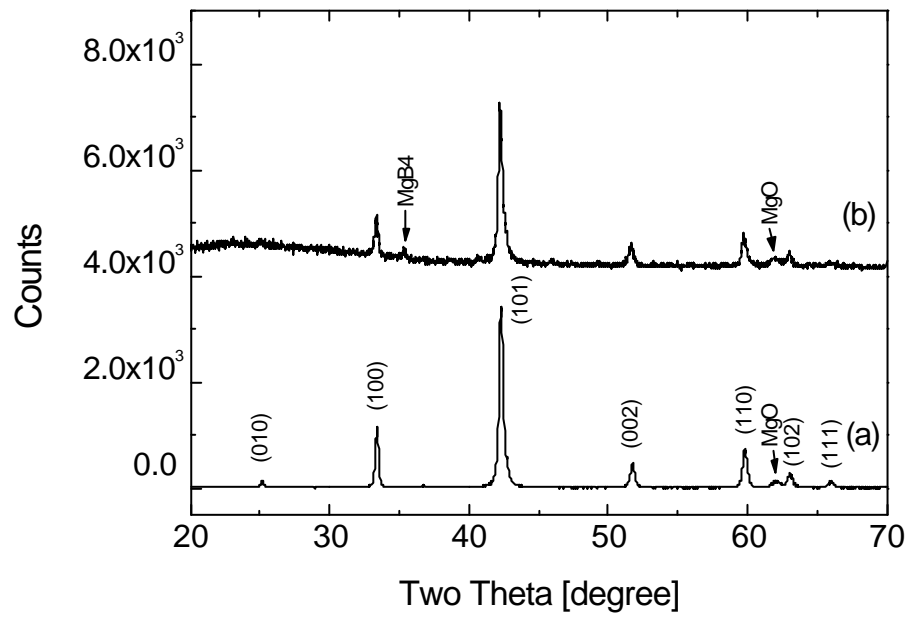


Fig. 2.

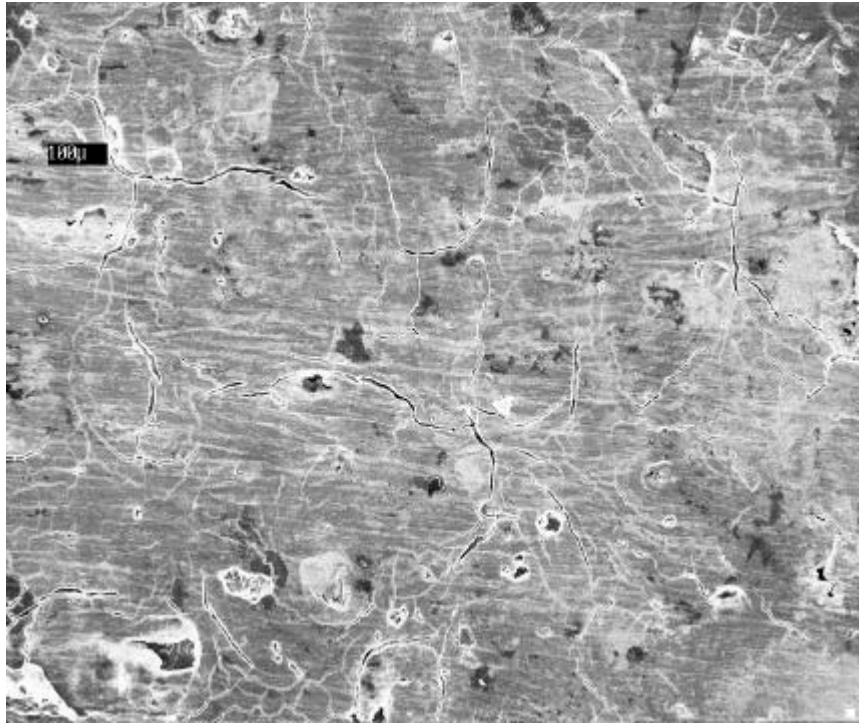


Fig. 3 (a)

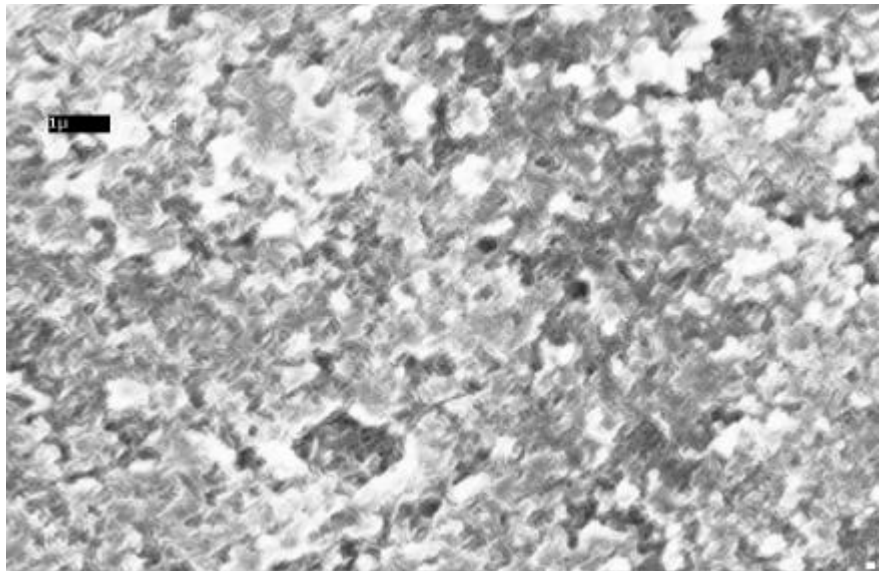


Fig. 3 (b).

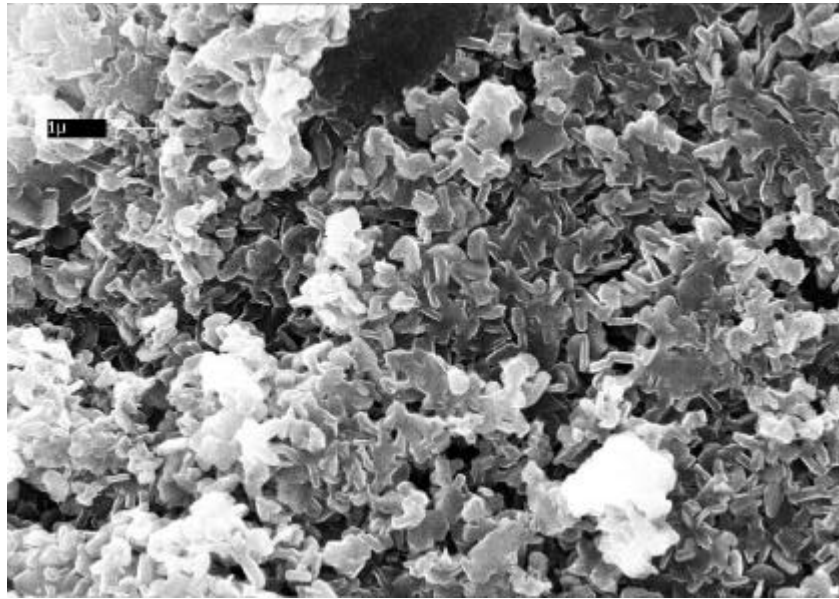


Fig. 3(c).

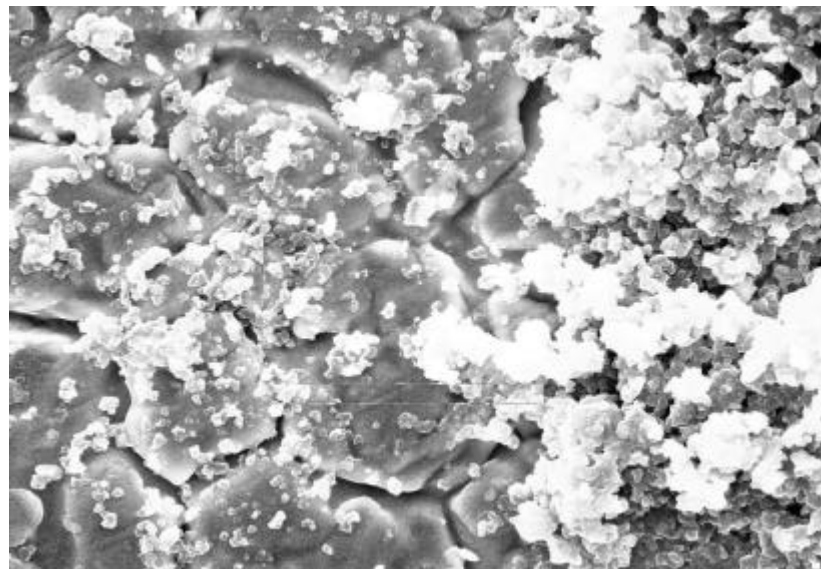


Fig. 3(d).

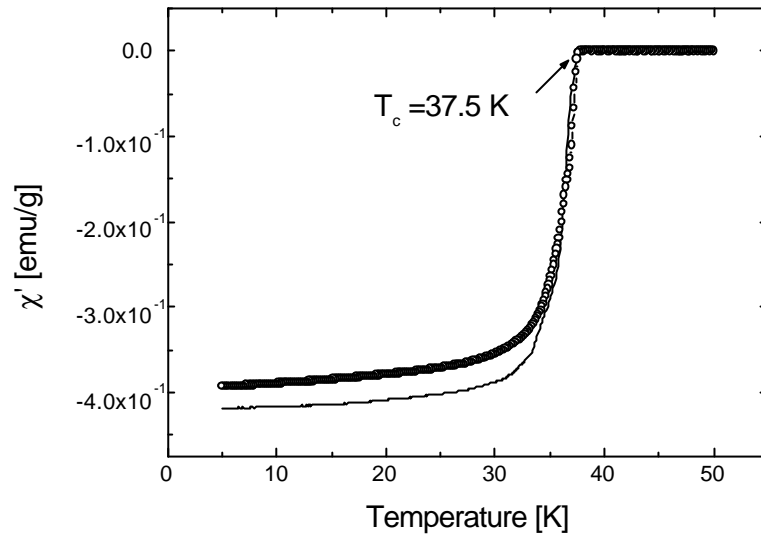


Fig. 4.

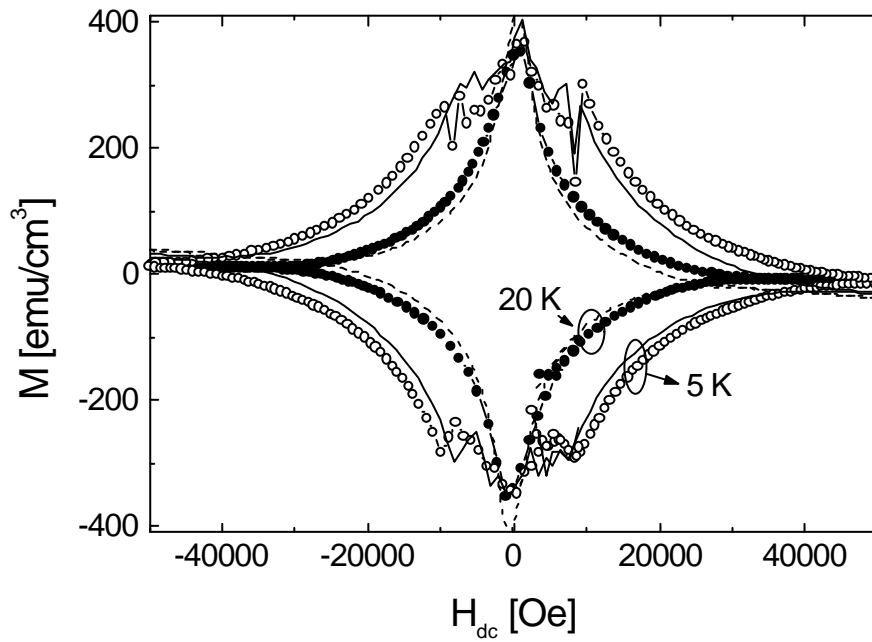


Fig. 5.

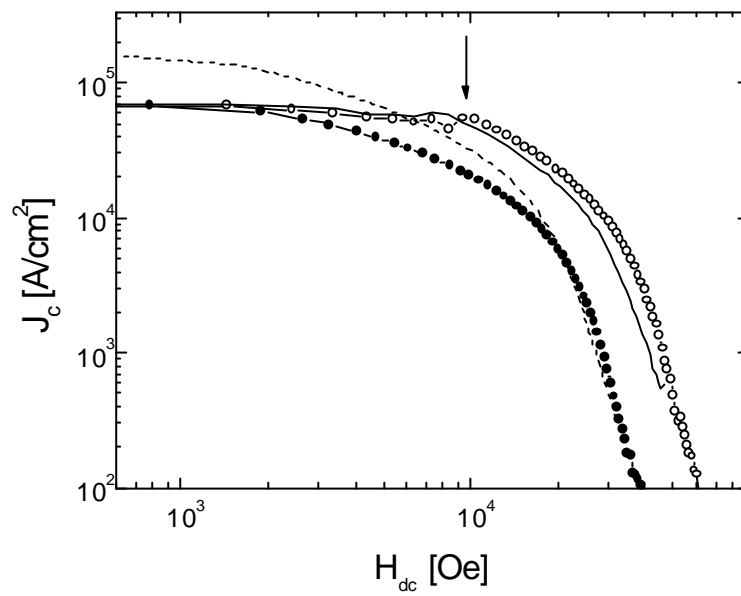


Fig. 6.